A Novel High Pressure, High Space Charge Capacity Ion Separation Device Based on Opposing Travelling Wave and DC potentials.

Authors: Martin Green; Keith Richardson; David Langridge; Thomas Moore
Affiliations: Waters Corporation, Wilmslow, UK

OVERVIEW

PURPOSE:

- Development of a novel separation device based on opposing T-Wave and DC field.
- Theoretical and experimental performance investigated.

METHOD:

- Analytical theory of operation developed.
- Prototype , 8 channel device tested in SYNAPT[TM]XS

RESULTS:

- IMS resolution ~45 FWHM (100ms scan) and charge capacity ~4E7 charges demonstrated.
- Demonstrated 'm/z' mode with high T-Wave velocity

INTRODUCTION

The utility of Travelling Wave Ion Mobility (TWIMS) in conjunction with Mass Spectrometers is well known. TWIMS has many advantages over DC field drift tubes. For example, length can be extended without increasing applied potentials, folded and closed loop devices may be constructed. However, performance is often compromised by limited charge capacity. Additionally, for fixed length, there is limited control over elution time without performance compromise.

Here we describe a new separation device, where RF confined ions are first trapped and then eluted using opposing Travelling Wave (TW) and DC potentials. This device is compact, has high space charge capacity, and allows easy control of elution time. In addition, altering conditions within the device allows substantially IMS or m/z like separation to be achieved.

METHODS

All experiments were performed using a modified Waters SYNAPT[TM] XS instrument **Figure 1**.
Ion current measurements were made using a Keysight[TM] B2985B Electrometer. Four phase TW was generated using An AIM-TTi TGA12104 Arbitrary waveform generator and Tabor Electronics 9400A four channel high voltage amplifier.

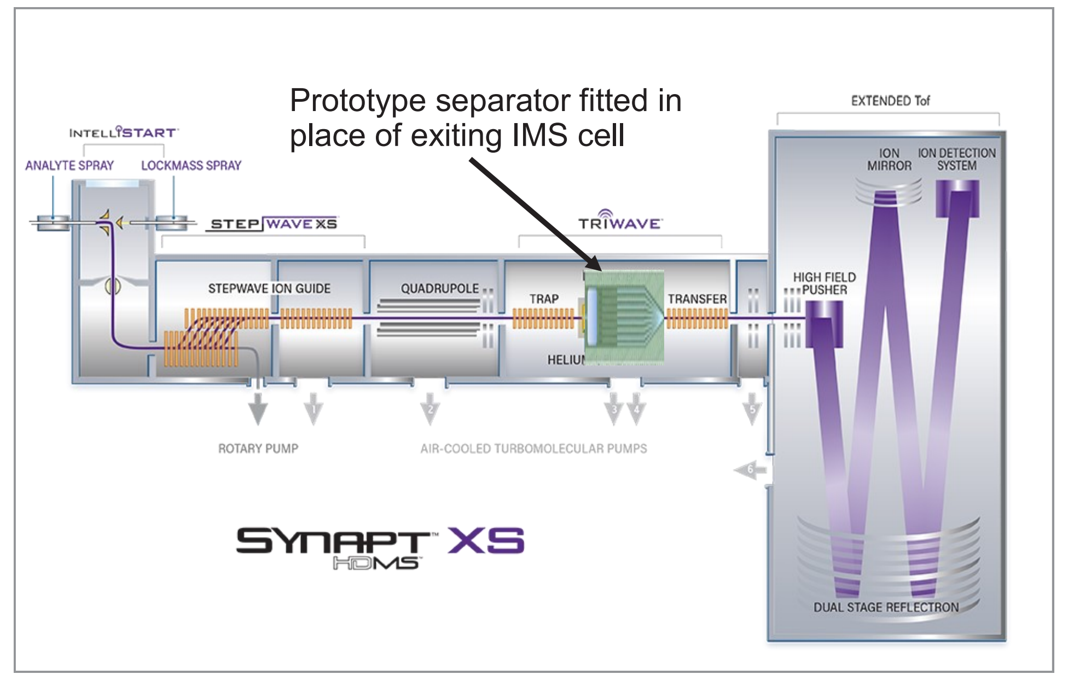

***Figure 1**. Prototype device installed in the TRIWAVE[TM] region of a Waters SYNAPT[TM] XS instrument*

Figure 1 shows the prototype separator installed in the TRIWAVE[TM] region of a Waters SYNAPT[TM] XS instrument.

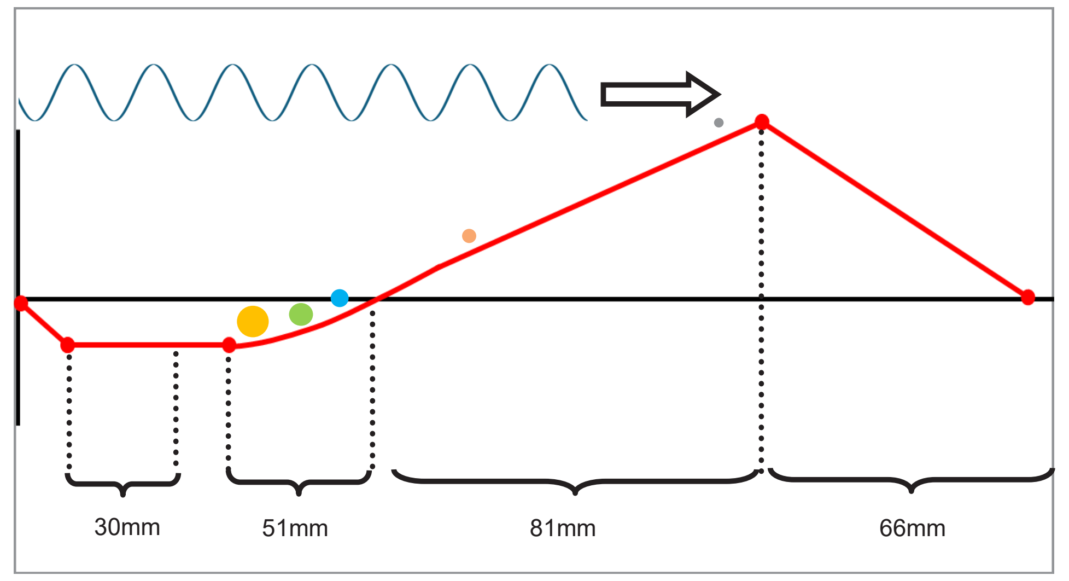

***Figure 2.** Dimensions and DC potential showing direction of T-Wave*

Figure 2 shows applied DC potentials. A 5x30x50mm pre-trapping region with no axial field is followed by 51mm trapping region with increasing axial field. This is followed by an 81mm analytical region with constant axial field. Finally, a 66mm funnel region is provided downstream. Both the trapping region and analytical region comprise 8 parallel 5mm diameter stacked ring ion guides (SRIG).

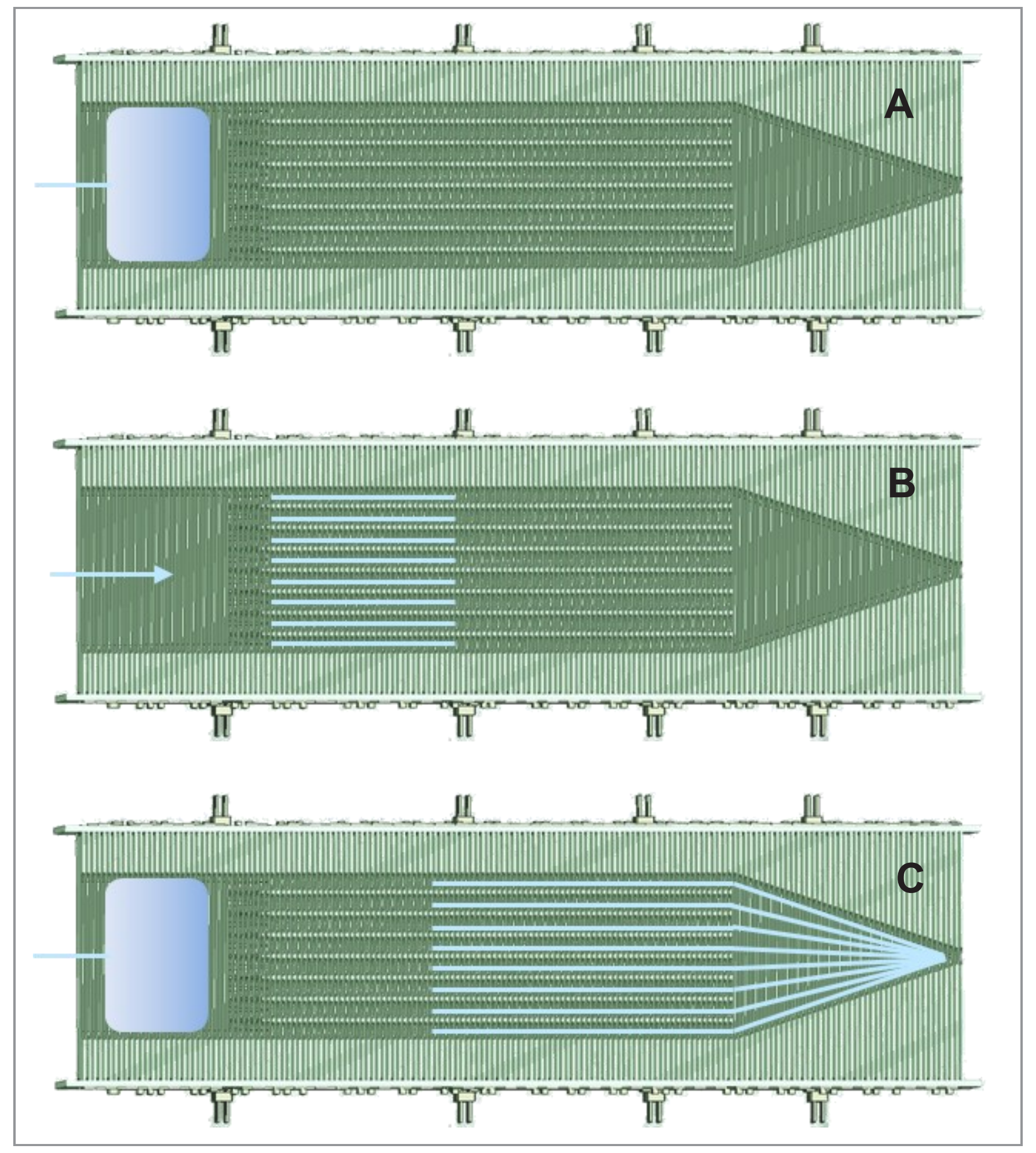

***Figure 3** **A**: Ions are accumulated in 30 x 50mm pre trap and allowed to distribute laterally. **B**: TW amplitude is increased and ions accumulate in parallel tunnel trapping region. **C**: T Wave amplitude is ramped to elute ions over analytical region. Ions from all tunnels are merged at end of funnel region.*

Figure 3 shows the mechanical construction and high duty cycle operation of the device. Ions enter a 5x30x50mm, field free pre-trap where they are free to distribute. A DC barrier is provided at the end of the pre-trap. The DC barrier is then removed and a TW is applied of sufficient amplitude to move ions into the 51mm long, 8 parallel tunnel trapping region (~5ms). The DC field in this region rises linearly causing ions of different properties (m/z and mobility) to take up different axial positions. Ions of low mobility reside closer to the start of the trapping region. The DC barrier is again applied to allow a second population to accumulate in the pre-trap. Simultaneously, the amplitude of the TW is ramped and ions elute over the analytical region and exit the device. Ions of high mobility / low m/z exit first.

The static DC field is supported by a series of resistor divider circuits and has a maximum of typically 1V/mm. A four phase, sinusoidal T Wave is capacitively coupled to all elements apart from a short region at the entrance and the exit ion funnel. The device was operated at a pressure of 1mbar N2 or 3mbar He.

THEORY OF OPERATION

In the pure mobility regime, the average ion velocity of an ion in a TW ion mobility device with a constant opposing DC electric field is approximately

$$\bar{v} = v\left(1-(1+\beta)\sqrt{1-g^2}\right) \qquad (1)$$

where *v* is the velocity of the travelling wave and *g* and β are dimensionless parameters that depend on ion properties, the electric field and the traveling wave parameters:

$$\beta = \frac{EK}{v} \qquad \gamma = 2\pi\frac{KV_0}{v\lambda} \qquad g = \frac{\gamma}{1+\beta}$$

E is the electric field strength, *K* is the ion mobility, V_0 is the TW amplitude on axis and *λ* is the wavelength. Note that *β* is the ratio of the DC-only drift velocity *EK* to the wave velocity *v*. When there is no applied DC, *β=1* and *g=γ* and standard travelling wave behavior is recovered[1]. Special values of *g* occur when ions are stationary (g_0):

$$g_0 = \sqrt{1-\frac{1}{(1+\beta)^2}}$$

and where they begin to "surf" at the wave velocity (*g=1*). The TW amplitude corresponding to the onset of surfing for an ion of mobility *K* is

$$V_S = \frac{(1+\beta)v\lambda}{2\pi K}$$

In the device described here, the TW amplitude ramps from an initial voltage V_i at a rate *r* i.e. $V_0(t)=V_i+rt$ leading to a time-dependent value for *g=g(t)*. Taking *E* to be the field in the analytical region, an ion reaches the end of the trapping region at time t_0 given by

$$t_0 = \frac{1}{r}(g_0 V_S - V_i) + \frac{1}{KE'(x)}$$

where *E'(x)* is the gradient of the electric field in the trapping region. The first term in this expression results directly from the balance condition, while the second part requires an explicitly time-dependent treatment and can be found by solving a convection-diffusion equation. The distance traveled through the analytical region at time *t* can be found by integrating (1):

$$x(t) = v(t-t_0) - \frac{v}{r}(1+\beta)V_S(a(t)-a(t_0))$$

where the dimensionless function *a(t)* is given by

$$a(t) = \frac{1}{2}g(t)(1-g^2(t)) - \tan^{-1}\frac{\sqrt{1-g^2(t)}}{1+g(t)}$$

For an analytical region of length *L*, these expressions can be used to find the transit time t_a. numerically The elution time for a given ion is then $t_{tot}=t_0+t_a$. In order to calculate mobility resolution, diffusion must be taken into account. It can be shown that in the trapping region, the width of the ion cloud for a given species is independent of time, wave parameters and ion mobility. The spatial standard deviation is

$$\sigma_x = \sqrt{\frac{k_B T}{zE'(x)}}$$

Where z is the charge state of the ion k_B is Boltzmann's constant and *T* is temperature. In the analytical region, diffusion continues normally (as in a standard drift cell or TW device). Although there is no simple general expression, when elution time is dominated by the trapping region, the resulting mobility resolution is approximately

$$R_K \simeq \frac{1}{2^{\frac{3}{8}}}\sqrt{\frac{z}{k_B T}}\left(\frac{\lambda}{2\pi}\right)^{\frac{1}{4}} E^{\frac{7}{8}}(Kv)^{\frac{1}{8}}\left(\frac{L}{r}\right)^{\frac{1}{4}}$$

RESULTS

Figure 4 shows the IMS resolution (CCS/ΔCCS) for a mixture of Raffinose and Melezitoze with 480m/s velocity TW, at 1mbar N2. Elution of a 3:1 mobility range in 100ms gave a FWHM resolution of ~45. For narrower mobility range and slower scans resolutions of ~120 FWHM have been achieved.

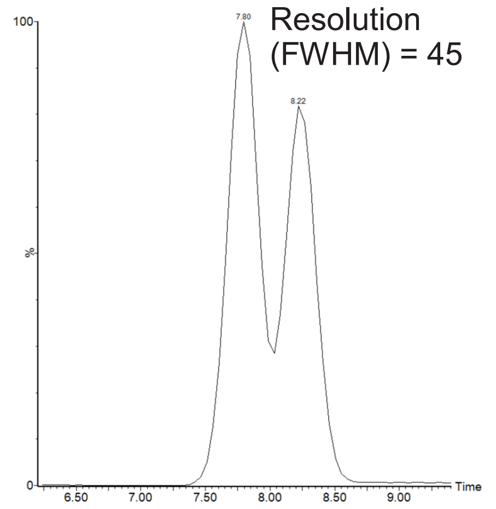

***Figure 4**. Raffinose Melezitose $[M+Na]^+$ = 572. 1 mbar N2, 480m/s T-Wave, 1V/mm DC field. 100ms scan time.*

Melazitoze CCS = 202.14Å^2

Raffinose CCS = 209.78 Å^2

Figure 5 shows a plot of intensity vs total charge in the device demonstrating a total charge capacity of ~ 4E7 and good linearity for species over an m/z range from 300—3000amu.

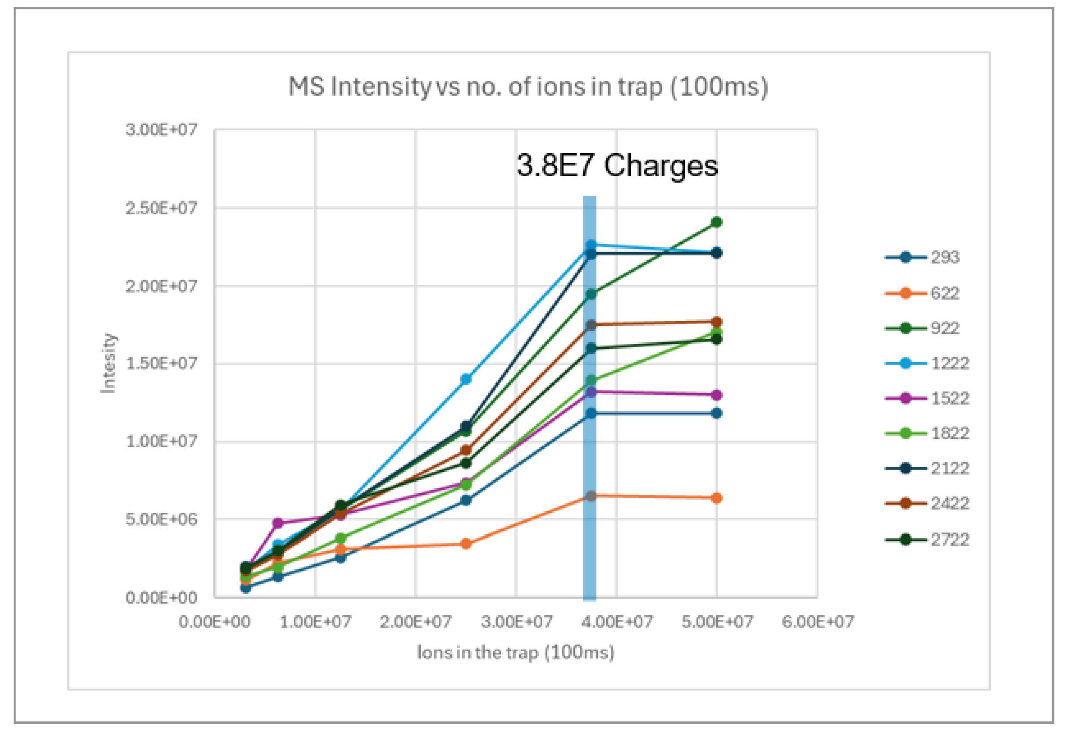

***Figure 5**. Intensity vs number of ions in the device for Agilent Test Mix showing good linearity up to a total charge capacity of ~4E7 charges.*

Figure 6. A shows the mass spectrum from an infusion of a Tryptic Digest of Alcohol dehydrogenase (ADH). The table shows the selected m/z values, and associated charge states, used to generate the arrival time distributions (ATD) in **Figure 6B and C**. **Figure 6B** shows ATD's for 100ms separation at 480m/s TW velocity. Under these conditions ions elute in order of ion mobility. Several peaks exhibit broadening or multiple maxima indicating ensembles of conformational states. **Figure 6C** Shows the ATD's for the same m/z values for a 100ms separation with a TW velocity of 1680m/s. Under these conditions the separation characteristic changes and ions elute in substantially m/z order.

At 1680m/s the peaks are significantly narrower as variation in conformational state is not reflected in the ATD. The peak capacity of the separation is significantly improved.

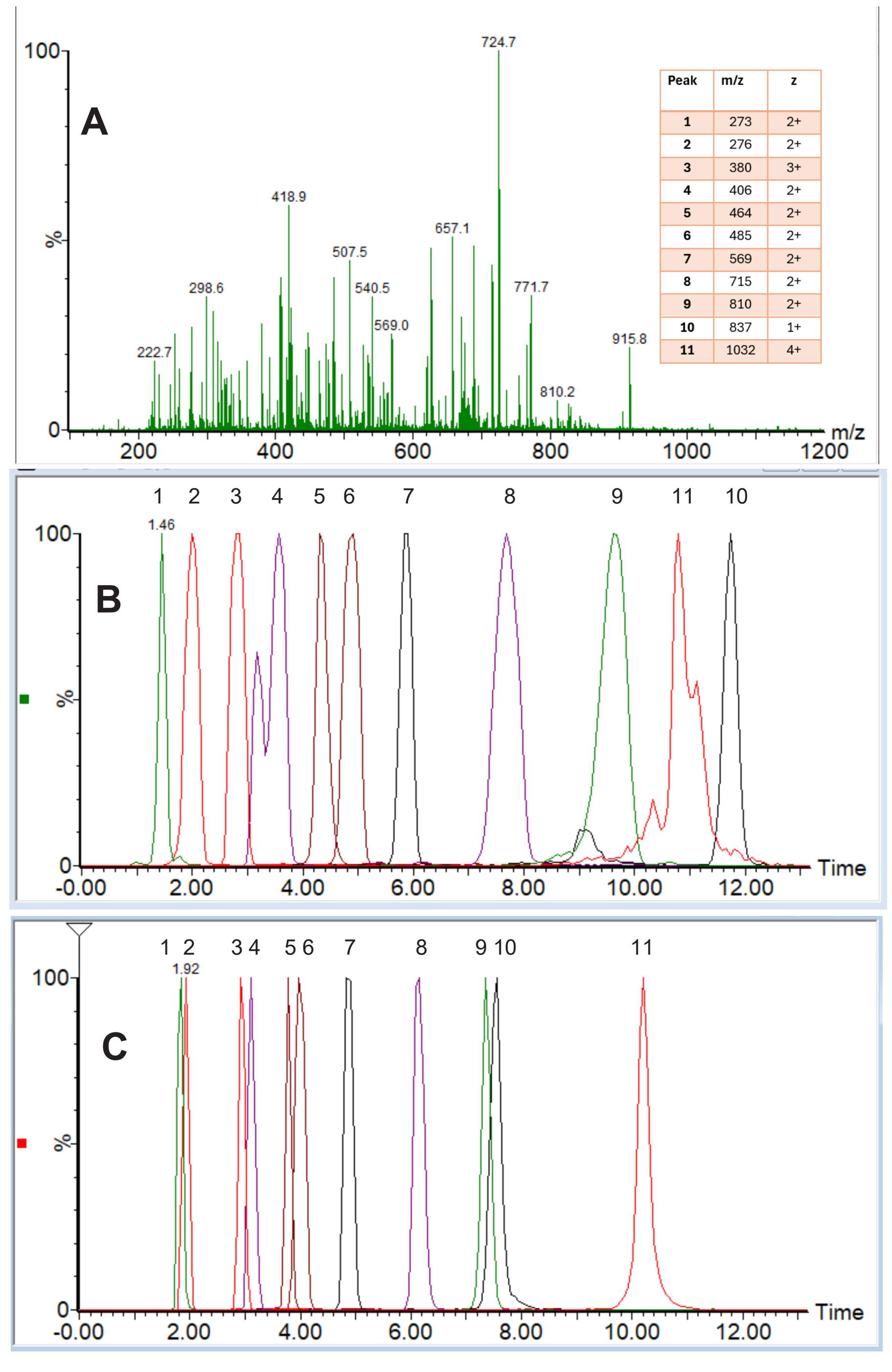

Peak	m/z	z
1	273	2+
2	276	2+
3	380	3+
4	406	2+
5	464	2+
6	485	2+
7	569	2+
8	715	2+
9	810	2+
10	837	1+
11	1032	4+

***Figure 6**. **A:** Mass spectrum of infusion of ADH Tryptic Digest and table of selected m/z values. **B:** ATD's for the selected m/z values at 480m/s TW velocity showing mobility separation with several peaks exhibiting multiple conformational states. **C:** ATD's for the selected m/z values at 1680m/z TW velocity showing narrower ATD's and predominantly m/z separation.*

Figure 7 Show mobility and m/z calibration of Polyaniline z=1 with 5 small molecules spiked into solution. Data was taken with 3mbar He. Mobility calibration was of the form $\bar{v} = aK^b$

At 480m/s TW velocity **(A)** residual errors in CCS value for calibrant and small molecules were less than +/-2%. (calibration coefficient b = 0.68).

At a TW velocity of 1920m/s. (**B)** the residual error in CCS value for the small molecules were as high as 17%. (calibration coefficient b = 0.675)

Calibrating directly in m/z, with a third order polynomial, at a TW velocity of 1920m/s (**C)** gave residual error in m/z of less than +/- 1%. Comparison of calibration errors **B** and **C** at 1920m/s demonstrates m/z separation dominating at the higher TW velocity.

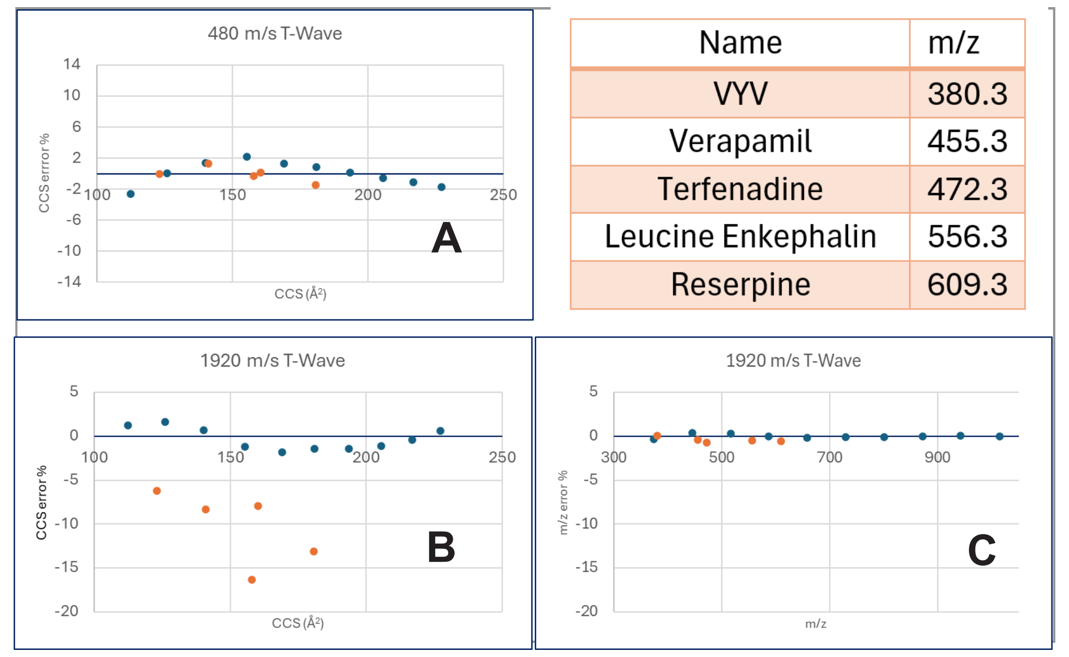

Name	m/z
VYV	380.3
Verapamil	455.3
Terfenadine	472.3
Leucine Enkephalin	556.3
Reserpine	609.3

***Figure 7**. **A:** Polyaniline mobility calibration TW 480m/s. **B:** Polyaniline mobility calibration TW 1920m/s. **C:** Polyaniline m/z calibration TW 1920m/s. Data in orange small molecules shown in inset table.*

DISCUSSION

This proof of principle prototype demonstrates the basic principles of operation of this novel device. The number of parallel channels is easily scalable to increase charge capacity and further improvements to resolution are envisaged including increasing the field within, or length of, the analytical region, and operating with lighter buffer gasses such as H2. The flexibility to vary operation continuously between mobility and m/z separation modes using TW velocity and amplitude is unique to this device and opens up previously unexplored operational modes.

The analytical approach presented has also been extended to account for the transition from IMS to m/z separation at higher T-Wave velocity.

This flexibility, peak capacity and high charge capacity makes this an ideal candidate for synchronization with a down-stream analytical quadrupole to improve the MS/MS duty cycle for DDA and DIA MS/MS[1].

CONCLUSION

- **Theoretical treatment and practical implementation of TW vs DC field separator show good agreement.**
- **Compact design capable of mobility resolution of ~45 in 100ms and charge capacity of ~4E7 charges.**
- **Novel m/z separation mode demonstrated at higher TW velocity.**
- **Future work includes :**
  - **Scaling number of channels for higher capacity**
  - **Optimizing / Increasing resolution**
  - **Positioning up stream of analytic quadrupole for high duty cycle MS/MS.**

References

1. Fundamentals of travelling wave ion mobility revisited: I. Smoothly moving waves. K. Richardson, D. Langridge, K. Giles, Int. J. Mass Spectrom. 428, 71-80 (2018)
2. Novel Operating Modes of an Ion Mobility Quadrupole Time-Of-Flight Hybrid Instrument; Wildgoose et. al. Proceedings of the 63rd ASMS, Conference on Mass Spectrometry and Allied Topics 2015, St Louis, Missouri.

Disclosure: The Authors are presenting this work as employees of Waters Corporation.

720008857EN